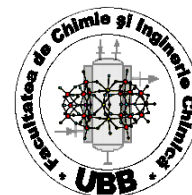




Babes-Bolyai University
Faculty of Chemistry and Chemical Engineering



Ph.D. Thesis

Timea ZOLTÁNI (MIHÁLY)

Coordination compounds of platinum(II) and palladium(II) with adenine derivatives

Scientific Advisors:

Prof. Dr. Ionel Haiduc

Prof. Dr. Ioan Silaghi-Dumitrescu[†]

CLUJ-NAPOCA
2013

Scientific committee:

Scientific advisors: Prof. Dr. Ionel Haiduc, Babes-Bolyai University, Cluj-Napoca
Prof. Dr. Ioan Silaghi-Dumitrescu, Babes-Bolyai University, Cluj-Napoca

President: Prof. Dr. Luminița Silaghi-Dumitrescu, Babes-Bolyai University, Cluj-Napoca

Reviewer: Prof. Dr. Bernhard Lippert, Technical University Dortmund, Dortmund

Reviewer: CSI Dr. Otilia Costișor, Institute of Chemistry Timișoara of Romanian Academy, Timișoara

Reviewer: Assoc. Prof. Dr. Edit Forizs, Babes-Bolyai University, Cluj-Napoca

Date of defence: 13th July 2013

Table of contents (full thesis)

Acknowledgements	5
Aim of the thesis	11
PART I.	
Di- and trinuclear complexes of 9-methyladenine with monofunctional palladium(II) and platinum(II) entities.....	12
Chapter 1. Literature overview of the nucleobase chemistry	14
1.1. Metal–nucleobase interactions	14
1.2. Coordination compounds of adenine and its derivatives.....	21
Chapter 2. Synthesis and characterization of new di- and trimetalated 9-methyladenine complexes containing platinum(II) and palladium(II)	30
2.1. Results and discussion.....	31
2.1.1. Synthesis of [Pt(NH₃)₃(9-MeA-<i>N</i>7)](ClO₄)₂ (11), [Pt(dien)(H₂O)] (ClO₄)₂ (12), [Pd(dien)(H₂O)](ClO₄)₂ (13), and [Pd(trpy)(H₂O)](ClO₄)₂ (14) as starting compounds ..	31
2.1.2. Synthesis and characterization of [(dien)Pd(<i>NI</i>-9-MeA-<i>N</i>7)Pt(NH₃)₃](ClO₄)₄·9.33H₂O (15).....	34
2.1.2.1. Synthesis of 15 on NMR and preparative scales.....	34
2.1.2.2. Molecular structure of 15	35
2.1.2.3. Solution behavior of 15	41
2.1.2.4. ¹⁹⁵ Pt NMR spectrum of 15	50
2.1.2.5. ESI-HRMS of complex 15	51
2.1.3. Synthesis and characterization of [(dien)Pt(<i>NI</i>-9-MeA-<i>N</i>7)Pt(NH₃)₃](ClO₄)₄·H₂O (16).....	52
2.1.3.1. Synthesis of 16 on NMR and preparative scales.....	52
2.1.3.2. Molecular structure of 16	53
2.1.3.3. Solution behavior of 16	55
2.1.3.4. ¹⁹⁵ Pt NMR spectrum of 16	60
2.1.4. Synthesis and characterization of [{Pd(trpy)}₂(<i>NI</i>,<i>N</i>6-9MeA-<i>N</i>7)Pt(NH₃)₃](ClO₄)₅·3H₂O (17)	62
2.1.4.1. Synthesis of 17 on NMR and preparative scales.....	62
2.1.4.2. Molecular structure of 17	63
2.1.4.3. Solution behavior of 17	66
2.1.5. DFT calculations on complexes 15, 17 and 18	68

2.2. General conclusions	74
2.3. Experimental part	75
2.3.1. General comments	75
2.3.2. Synthesis of original compounds	77
2.3.2.1. [(dien)Pd(<i>NI</i> -9-MeA- <i>N7</i>)Pt(NH ₃) ₃](ClO ₄) ₄ ·9.33H ₂ O (15)	77
2.3.2.2. [(dien)Pt(<i>NI</i> -9-MeA- <i>N7</i>)Pt(NH ₃) ₃](ClO ₄) ₄ ·H ₂ O (16)	79
2.3.2.3. [{(trpy)Pd} ₂ (<i>NI,N6</i> -9-MeA- <i>N7</i>)Pt(NH ₃) ₃](ClO ₄) ₅ ·3H ₂ O (17)	81
REFERENCES I	83
PART II.	
On the reactivity of platina-β-diketone towards nucleobases: a new way to platinum complexes of adenine and its derivatives	86
Chapter 3. Literature overview on the chemistry of platina-β-diketone	88
Chapter 4. Synthesis, characterization and reactivity of new adenine based aminocarbene platinum(II) complexes	101
4.1. Results and discussion	101
4.1.1. Synthesis and characterization of adenine based aminocarbene Pt^{II} complexes [Pt(COMe)Cl{CMe(<i>N6-R,9-R'</i>A⁻)-κC,κN}] (32–36)	101
4.1.1.1. Synthesis of complexes 32–36	101
4.1.1.2. Molecular structure of complexes 32 and 34	102
4.1.1.3. ¹ H NMR spectra of complexes 32–36	105
4.1.1.4. ¹⁹⁵ Pt spectra of complexes 32, 34 and 36	108
4.1.1.5. ¹³ C NMR spectrum of complex 36	108
4.1.1.6. ESI-FTICR-MS of complexes 32–36	110
4.1.1.7. DFT calculations of complexes 32–36	111
4.1.2. Synthesis and characterization of Pt^{II} containing ketoimine complexes	115
4.1.2.1. Synthesis of [Pt(EtNH ₂)Cl{(COMe){C(N-Et)Me}H}] (37) and [Pt(<i>i</i> -PrNH ₂)Cl{(COMe){C(N- <i>i</i> -Pr)Me}H}] (38)	115
4.1.2.2. ¹ H NMR spectra of complexes 37 and 38	116
4.1.2.3. ¹⁹⁵ Pt spectra of complexes 37 and 38	120
4.1.2.4. ¹³ C NMR spectra of 37 and 38	120
4.1.2.5. ESI-FTICR-MS of complexes 37 and 38	126
4.1.2.6. DFT calculations of 37 and 38	126
4.2. General conclusions	131

4.3. Experimental section.....	132
4.3.1. General comments	132
4.3.2. Synthesis of original compounds	134
4.3.2.1. [Pt(COMe)Cl{CMe(<i>N</i> 6-R, <i>N</i> 9-R' <i>A</i> ⁻)-κC,κN}] (32–36)	134
4.3.2.2. [Pt(RNH ₂)Cl{(COMe){C(NR)Me}H}] (37, 38).....	139
References II.....	141
Appendix I.	143
ESI-FTICR-MS of complexes 32–38	143
Appendix II.....	147
Atomic coordinates of complexes 15, 17, and 18	147
Appendix III.	154
Atomic coordinates of complexes 32'–38'	154
List of synthesized compounds	169
List of publications related to this thesis.....	170
List of further publications	170
List of oral presentations related to this thesis.....	171
List of further presentations and posters.....	171

Aim of the thesis

The aim of this work represents the synthesis and characterization of new coordination compounds of adenine and its derivatives with transitional metals. The thesis is divided in two main parts, both of them containing two chapters.

Chapter 1 is intended to be a literature overview on the coordination chemistry of nucleobases, involving the history, the importances of this chemistry, and presenting the most relevant coordination modes of adenine and its derivatives (the molecular structures are drawn from the .cif files deposited at the *Cambridge Structural Database* “CSD”).

Chapter 2 presents original results of new two- and threefold metal coordination regarding monodentate metal entities (Pd^{II} and Pt^{II}) to *N1*, *N6*, and *N7* of 9-methyladenine (9-MeA) model nucleobase. Therefore, the synthesis and characterization of these complexes both in the solid state and in solution are being described. In the subchapter *Results and discussion*, some parts concerning the structural characterization and the solution behavior of the original complexes have been already published in the articles cited in the thesis.

The second part has the purpose to present the synthesis of platinum(II) containing adenine based aminocarbene complexes, using platina- β -diketone as Pt^{II} source.

Therefore, **Chapter 3** describes literature data regarding the chemistry of platina- β -diketones with different type of ligands. After an overview on the chemistry of the platina- β -diketone, **Chapter 4** presents the original results concerning the synthesis and reactivity of new aminocarbene type adenine complexes. In order to be able to study these aminocarbene adenine complexes, several adenine derivatives like 6,9-MeA, 9-MeA, adenosine, 2',3'-isopropylidene adenosine, were used. The obtained new aminocarbene complexes were characterized by NMR spectroscopy, ESI-FTICR-MS, and for two aminocarbene complexes X-ray crystal structures were determined. Furthermore, the reactivity of these aminocarbene complexes with alkyl amines was studied, yielding the first platinum- β -ketoimines. Furthermore, DFT calculations both on the aminocarbene complexes and on the platinum- β -ketoimines were carried out. Some parts of the original results are included in a scientific paper.

Both of **Part 1** and **Part 2** contain general conclusions on the obtained results, experimental part and references. The thesis ends with appendix, list of publications, and the published articles related to the thesis.

Abbreviations

A	adenine
G	guanine
T	thymine
C	cytosine
A⁻	adeninate anion (deprotonated at <i>N9</i>)
9-MeA	9-methyladenine
9-MeA⁻	9-methyladeninate anion (deprotonated at <i>N6</i>)
6,9-diMeA	6, 9-dimethyladenine
6,9-diMeA⁻	6, 9-dimethyladeninate anion (deprotonated at <i>N6</i>)
Ado	adenosine
Ado⁻	adenosine anion (deprotonated at <i>N6</i>)
<i>i</i>Pr-Ado	2',3'-isopropylidene-adenosine
<i>i</i>Pr-Ado⁻	2',3'-isopropylidene-adenosine anion (deprotonated at <i>N6</i>)
9-MeG	9-methylguanine
9-MeG²⁻	9-methylguaninate anion (deprotonated at <i>N1</i> and <i>N2</i>)
6-MeA⁻	6-methyladeninate anion (deprotonated at <i>N9</i>)
py	pyridine
bpy	2,2'-bipyridine
4,4'-<i>t</i>-Bu₂-bpy	4,4'-di- <i>t</i> -buthyl-2,2'-bipyridine
4-Mepy	4-methylpyridine
dien	diethylenetriamine
trpy	2,2',6',2''-terpyridine
diMeCarb	dimethylcarbamide
dppe	bis(1,2-diphenylphosphino)ethane
H₂dmg	dimethylglyoxime
pydz	pyridazine
Hacac	acetylacetone
EtNH₂	ethylamine
<i>i</i>-PrNH₂	isopropylamine
BnNH₂	benzylamine

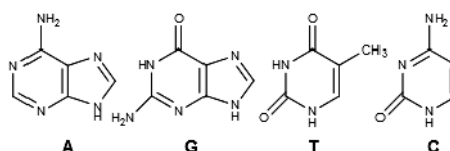
Keywords: 9-methyladenine, migration, monofunctional, di- and trimetalated species, aminocarbene complex.

Part I

Di- and trinuclear complexes of 9-methyladenine with monofunctional palladium(II) and platinum(II) entities

Chapter 1. Literature overview of the nucleobase chemistry

The nucleic acid chemistry has been started in 1860s, following to the isolation of a substance from human pus cells by Friedrich Miescher what he called ‘nuclein’. This material was a mixture of nucleic acids and proteins [1]. In 1953, James D. Watson and Francis Crick established the structure of DNA, a double helix of antiparallel strands in which the complementary purine and pyrimidine bases are held together by hydrogen bonds [2]. The **Scheme 1** shows the purine (adenine (A), guanine (G)) and pyrimidine bases (thymine (T), cytosine (C)) of DNA.

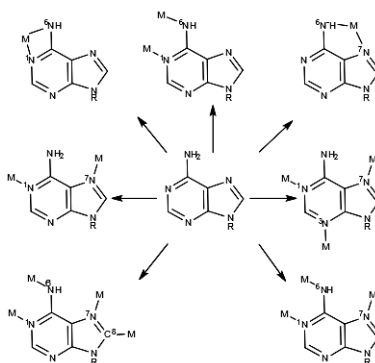


Scheme 1.

In the late 1960s, B. Rosenberg discovered the antitumor properties of *Cisplatin* (*cis*-[Pt(NH₃)₂Cl₂]), which is based on its interaction with cellular DNA, leading to the formation of various types of adducts [3]. Following the discovery that Pt^{II} – DNA adducts can block the replication of DNA and kill tumor cells [4], the metal – nucleic acid studies became one of the most interesting topics in bioinorganic metal coordination chemistry. The antitumor activity of *Cisplatin* stimulated the search for new anticancer active metal compounds with similar properties, but toxicities as low as possible [5].

On the one hand, metal species can interact with nucleic acids directly *via* N, O, and C donor atoms of nucleobases, oxygen atoms of sugar, or of the phosphate part, and combinations of them. On the other hand the metal DNA interactions can be realized indirectly *via* hydrogen bonds, $\pi - \pi$ interactions between a co-ligand of the metal complex and the nucleobases, or weak forces such as van der Waals interactions [6].

The *N9*-blocked adenine at physiological *pH* contains three unprotonated endocyclic nitrogen atoms (*N1*, *N3*, *N7*), as potential metal coordination sites. Depending upon the specific conditions (*pH*, ratio of metal : nucleobase, nature of the metal) binding to any of these positions, either *individually* or in *pairwise* combinations, is possible (**Scheme 2**) [6].



Scheme 2 [6].

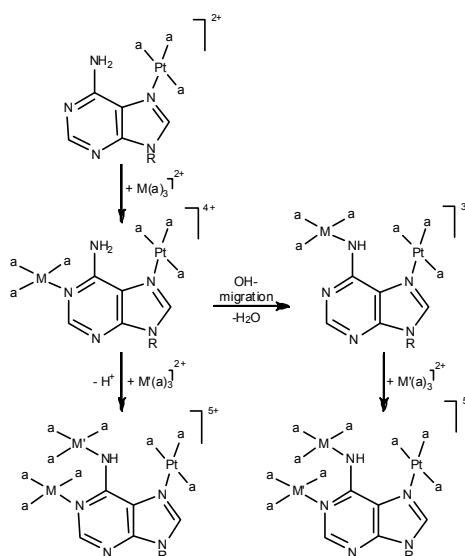
More than 30 years ago was found in the 9-blocked-adenine systems (e.g. 9-MeA) that the *N1* donor atom is the preferred metal coordination site [7]. The coordination *via N3* atom can be also realized when the *N1* and *N7* atoms are blocked by the methylation of the exocyclic NH_2 group [8]. In addition, metal binding to the exocyclic *N6* position is possible, following deprotonation of this site or a shift of proton from the exocyclic amino group to an endocyclic ring nitrogen atom (e.g. *N1*), hence tautomerization. Therefore, it is not necessary strongly alkaline media [9]. The formation of *N6* metalated species can be realized also by an initially metal coordination to *N1* or *N7*, followed by metal migration. Arpalahti has demonstrated the migration of metal ion from *N1* to *N6* [10]. In 1975 the first complex of 9-MeA coordinating *via N1* atom was synthesized and characterized. The crystal structure analysis of a zinc-(9-MeA) complex has shown that in slightly acidic media, the *N1* atom of 9-MeA is a strong binding site and being preferred over all other possible sites for divalent metal coordination to a purine base [11]. Lippert and collaborators were interested to prepare a Pt^{II} compound of 9-MeA, realizing the first Pt-N1 bond in 9-MeA systems [12]. One of the first complexes in which the 9-MeA ligand is coordinated *via N7* atom was prepared in the 1976 [13]. The connection of two adenine rings is possible, and also the coordination mode to platinum atoms *via N1* and *N7* was realized. Furthermore, the adenine ligands present a “head–head” orientation around the central platinum atom [14]. Moreover, two alkyladenine moieties bonded to metal ions *via* two N atoms, can adopt a “head–tail” orientation [15]. As a consequence of the near perpendicular vectors, molecular “squares” having *N1,N7*-dimetalated purine nucleobases can be obtained [16]. In complex $[PtMe_3\{(N1,N6,N7-9-MeA^-\})_3] \cdot Me_2CO$ the threefold metal binding pattern of the 9-MeA *via N1, N6, N7* donor atoms was realized [17].

Chapter 2.

Synthesis and characterization of new di- and trimetalated 9-methyladenine complexes containing platinum(II) and palladium(II)

The goal of this work was to understand the formation of a threefold metalated species of 9-MeA, with metals coordinated *via* *N1,N7,N6* atoms. The formation of trimetalated species was observed accidentally when reacting 9-MeA with an excess of $[\text{Pd}(\text{dien})(\text{OH})]^+$ at *pH* 11 [18a]. In order to find a better understanding of the mechanism, in complex $[\{\text{Pd}(\text{dien})\}_3(9\text{-MeA}^- - \text{N1}, \text{N6}, \text{N7})]\text{Cl}_{3.5}[\text{PF}_6]_{1.5} \cdot 3\text{H}_2\text{O}$ (18) [18] (see below), the labile $\text{Pd}^{\text{II}}(\text{dien})$ units were replaced partially by more inert Pt^{II} entities, namely $\text{Pt}^{\text{II}}(\text{NH}_3)_3$ and $\text{Pt}^{\text{II}}(\text{dien})$.

This study is based on previously findings of Lippert and coworkers [19], especially that blockage of the *N7* position of 9-MeA by $\text{Pt}^{\text{II}}(\text{NH}_3)_3$ permits a more detailed study of the coordination chemistry of pyrimidinic part of the purine nucleobase [19a]. Thus, it was of interest to find out whether the formation of a trimetalated 9-MeA species occurs directly from a *N1,N7* dimetalated species or *via* a metal migration from *N1* to *N6*, followed by a remetalation of *N1* (Scheme 3) [18].



Scheme 3.

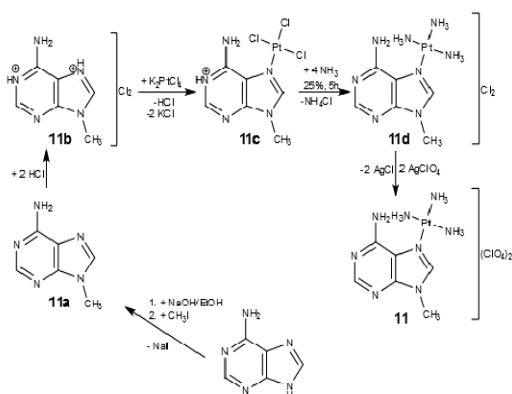
Therefore, several di- and trinuclear metal complexes consisting of the model nucleobase 9-MeA and monofunctional $\text{Pd}^{\text{II}}(\text{dien})$, $\text{Pt}^{\text{II}}(\text{dien})$, $\text{Pt}^{\text{II}}(\text{NH}_3)_3$, or $\text{Pd}^{\text{II}}(\text{trpy})$ in different combinations have been prepared and studied in solution by NMR spectroscopy: $[(\text{dien})\text{Pd}(\text{N1-9-MeA-N7})\text{Pt}(\text{NH}_3)_3](\text{ClO}_4)_4 \cdot 9.33\text{H}_2\text{O}$ (15), $[(\text{dien})\text{Pt}(\text{N1-9-MeA-}$

$N7)Pt(NH_3)_3](ClO_4)_4 \cdot H_2O$ (**16**), $[\{(trpy)Pd\}_2(NI, N6-9-MeA^- -N7)Pt(NH_3)_3](ClO_4)_5 \cdot 3H_2O$ (**17**).

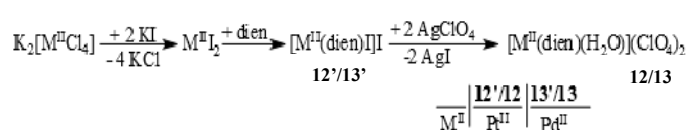
Synthesis of $[Pt(NH_3)_3(9-MeA-N7)](ClO_4)_2$ (11**), $[Pt(dien)(H_2O)](ClO_4)_2$ (**12**), $[Pd(dien)(H_2O)](ClO_4)_2$ (**13**), and $[Pd(trpy)H_2O](ClO_4)$ (**14**) as starting compounds**

In order to get an insight concerning the mechanism of the formation of treefold metalated species of 9-MeA, the $[Pt(NH_3)_3(9-MeA-N7)](ClO_4)_2$ (**11**) was applied as precursor complex, synthesized according to the literature method (**Scheme 4**) [20, 21, 22].

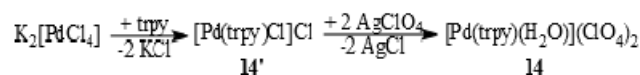
The syntheses of the further precursor complexes, namely $[Pt(dien)(H_2O)](ClO_4)_2$ (**12**) and $[Pd(dien)(H_2O)](ClO_4)_2$ (**13**) were started with the preparation of complexes **12'** and **13'** having the general formula $[M^{II}(dien)I]I$ ($M^{II} = Pt^{II}/Pd^{II}$; **12'/13'**), according to the published method for the complex **12'** [23]. Furthermore, the activation of **12'** and **13'** took place using an aqua solution of $AgClO_4$ (**Scheme 5**). Complex **14** was obtained by the activation of complex $[Pd(trpy)Cl]Cl$ (**14'**) [24] with an aqueous solution of $AgClO_4$. The synthetic route for complex **14** is presented in the **Scheme 6**.



Scheme 4.



Scheme 5.

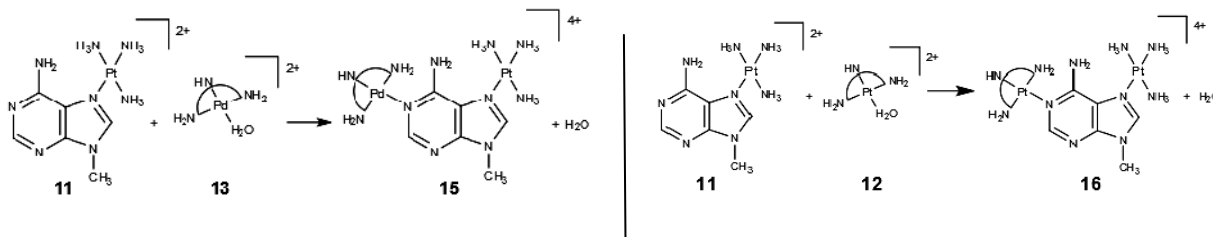


Scheme 6.

Synthesis of $[(dien)Pd(NI-9-MeA-N7)Pt(NH_3)_3](ClO_4)_4 \cdot 9.33H_2O$ (15**) $[(dien)Pt(NI-9-MeA-N7)Pt(NH_3)_3](ClO_4)_4 \cdot H_2O$ (**16**) and $[\{Pd(trpy)\}_2(NI, N6-9MeA-N7)Pt(NH_3)_3](ClO_4)_5 \cdot 3H_2O$ (**17**)**

Complex $[(dien)Pd(NI-9-MeA-N7)Pt(NH_3)_3](ClO_4)_4 \cdot 9.33H_2O$ (**15**) was prepared by reacting $[Pt(NH_3)_3(9-MeA-N7)](ClO_4)_2$ (**11**) with an excess of $[Pd(dien)(H_2O)](ClO_4)_2$ (**13**) in water (**Scheme 7**) [18]. In contrast to complex **15**, complex $[(dien)Pt(NI-9-MeA-$

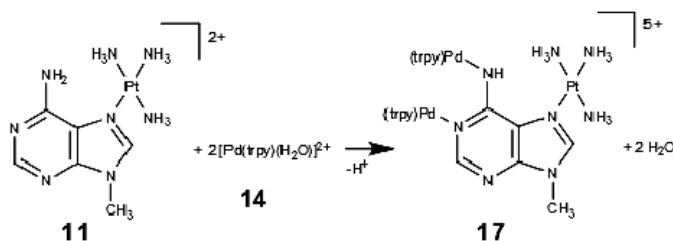
$N7Pt(NH_3)_3](ClO_4)_4 \cdot H_2O$ (**16**) was prepared by reacting $[Pt(NH_3)_3(9-MeA-N7)](ClO_4)_2$ (**11**) with $[Pt(dien)(H_2O)](ClO_4)_2$ (**12**) in 1:1 and 1:2 ratio (**Scheme 8**).



Scheme 7.

Scheme 8.

Complex $\{[Pd(trpy)]_2(N1,N6-9MeA-N7)Pt(NH_3)_3\}(ClO_4)_5 \cdot 3H_2O$ (**17**) was prepared by reacting $[Pt(NH_3)_3(9-MeA-N7)](ClO_4)_2$ (**11**) with $[Pd(trpy)(H_2O)](ClO_4)_2$ (**14**) in water (**Scheme 9**). Complex **17** was obtained using the precursor complexes (**11:14**) in 1:1, 1:2, and 1:3 ratio.

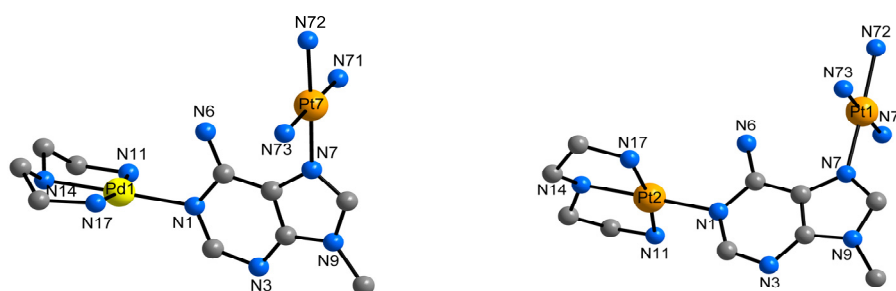


Scheme 9.

In order to find out the optimal reaction conditions to obtain the complexes **15** – **17**, several experiments were done on NMR scale. Therefore, different molar ratios of the reactants were used; the pH of the solutions was adjusted; the optimal temperature and reaction time were also tested.

Molecular structures of **15** and **16**

Both closely similar cations of $[(dien)Pt(N1-9-MeA-N7)Pt(NH_3)_3](ClO_4)_4 \cdot H_2O$ (**16**) $[(dien)Pd(N1-9-MeA-N7)Pt(NH_3)_3](ClO_4)_4 \cdot 9.33H_2O$ (**15**) presented in **Figure 1**, differ in water content (crystal packing), space groups of the unit cells, namely R-3 (**15**) and P-1 (**16**).

Figure 1. Cations of complex **15** (left) and **16** (right).

In the crystal, cations of **16** are surrounded by a water molecule and nine perchlorate anions. Two of them interact *via* twofold anion– π interactions with both adenine rings (**Figure 2**) [18].

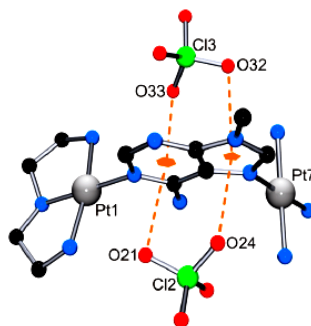


Figure 2. Twofold anion– π interactions in **16**.

The remaining perchlorate anions are involved in hydrogen bonds with cation **16**. Furthermore, no significant interactions between cations are observed.

Crystal packing of **15** is governed by hydrogen bond interactions between $[(\text{dien})\text{Pd}(\text{N1-9-MeA-N7})\text{Pt}(\text{NH}_3)_3]^{4+}$ cations, ClO_4^- ions and water molecules. Therefore, the different NH_3 , NH_2 , and NH sites of cation **15** participate as donors, while the ClO_4^- counter anions and some water molecules are the hydrogen bond acceptors. Although, in principle, the N3 site of **15** could act as a hydrogen bond acceptor site, crystal packing of **15** shows that N3 is not involved in such interactions. The crystal packing of complex **15**, forming a honeycomblike lattice with hexagonal tunnels is shown in **Figure 3**.

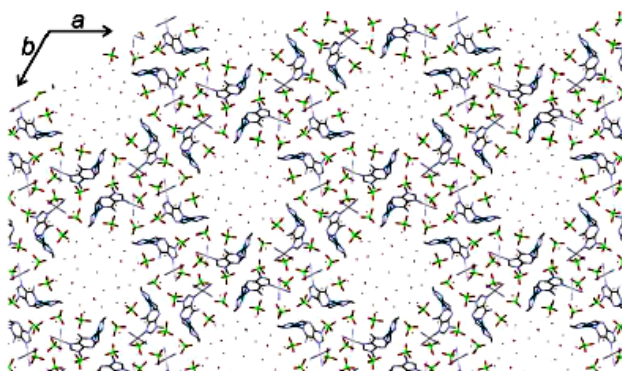


Figure 3. View of the packing of **1** along the b axis, forming a honeycomblike lattice with hexagonal tunnels.

In the asymmetric unit of complex **15**, 11 crystallographically different water molecules ($\text{O1w} - \text{O11w}$) are observed. Four water molecules (O1w , O2w , O3w , and O4w) are directly hydrogen bonded to the cation **15**, and O4w is part of the water cluster tubular skeleton (see below). A 12-atoms crown defined by six hexagon-shared O8w , and six bridging O9w atoms represent the nanotube inner cavity section (shaded region of **Figure 4**).

Subsequently, a total of 30 water molecules are involved; six of them (O8w) shared between hexagons ($-O8w-O9w-O8w'-O6w-O7w-O4w-$) adopting a distorted chair conformations. Fused hexagons presented in **Figure 4** display mutual *up,down,up,down,up,down* dispositions (*e.g.* position of O8w). Water molecules of this crown lie on four different parallel planes (and perpendicular to the *c* axis), as illustrated in **Figure 5**. Six symmetry related O5w atoms cross-link two alternate up-disposed hexagons ($O5w \cdots O6w$, 2.93(3) Å; $O5w \cdots O7w'$, 2.70(3) Å) to a down-disposed hexagon (or *vice versa*) of a neighboring unit, resulting in a 10-atom closed water cluster ($-O5w-O6w-O8w-O9w-O8w-O4w-O7w-O5w-O6w-O7w-$), which shares several edges with the fused-hexagon blocks (**Figure 6**). However, the nanotube is not chiral and no formation of internal helices is observed. A representation of this single-walled water cluster nanotube is presented in **Figure 7**.

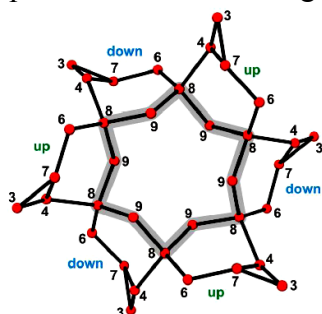


Figure 4. Projection view on the *ab* plane of the water cluster nanotube in 15. Numbers represent water molecule numbering (*i.e.*: 8, O8w). Shaded region represents the nanotube inner cavity section.

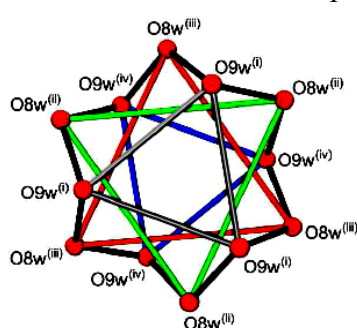


Figure 5. Upper view (from the *c* axis) of the central water cluster crown in 15. Triangles represent planes *i-iv*.

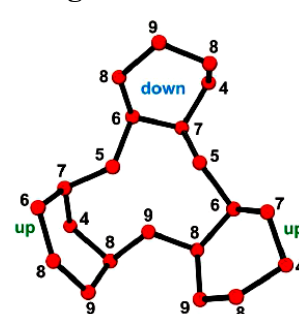


Figure 6. Detailed view of connection between up- and down-disposed hexagons of the water cluster nanotube in 15. Numbers represent water molecule numbering (*i.e.*: 5, O5w).

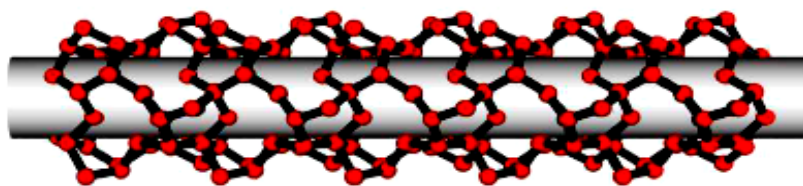


Figure 7. Representation of the single-walled water cluster infinite nanotube of 15 along the *c* axis.

Molecular structure of 17

From the reaction of complexes **11** and **14** on preparative scale, orange suitable crystals of **17** were isolated. **Figure 8** gives two views of the molecular cation of **17**.

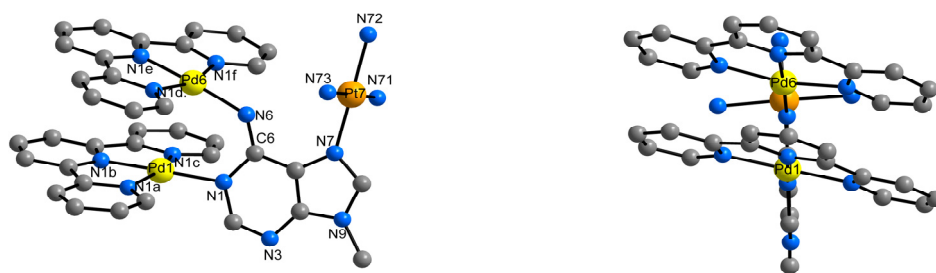


Figure 8. Molecular cation of 17.

Cation **17** displays an analogous binding pattern as $[\{\text{Pd}(\text{dien})\}_3(9\text{-MeA}^- \text{N1,N6,N7})\text{Cl}_{3.5}(\text{PF}_6)_{1.5}\cdot 3\text{H}_2\text{O}$ [**18**], with $\text{Pt}^{\text{II}}(\text{NH}_3)_3$ at *N7* (*Pt7*) and two $\text{Pd}^{\text{II}}(\text{trpy})$ units at *N1* (*Pd1*) and *N6* (*Pd6*), in place of the three $\text{Pd}^{\text{II}}(\text{dien})$.

Solution behavior of 15

Complex **15**, when dissolved in D_2O ($\text{pD} = 5.8$ at $c \approx 5 \cdot 10^{-3}$ M), partially dissociates into the Pt starting complex $[\text{Pt}(\text{ND}_3)_3(9\text{-MeA-N7})]^{2+}$ (**11**) and $[\text{Pd}(\text{dien})(\text{D}_2\text{O})]^{2+}$ (**13**) (Scheme 10) [**18**]. This dissociation is proved by the ^1H NMR spectrum of complex **15** ($\text{pD} = 5.8$ at $c \approx 5 \cdot 10^{-3}$ M), shown in the Figure 9.

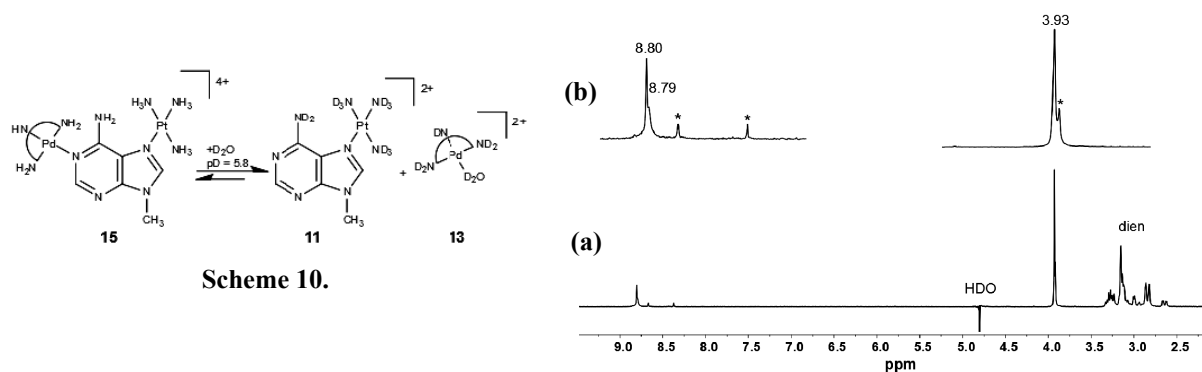


Figure 9. ^1H NMR spectra of **15** in D_2O :
 (a) Overview spectrum, $c = 5 \cdot 10^{-3}$ M, $\text{pD} = 5.8$;
 (b) Details of aromatic and CH_3 resonances of spectrum (a).

In order to find out whether the signals of the **11** starting compound are due to an impurity or due to a dissociation process, more experiments were done. First of all, the concentration dependent ^1H NMR spectra were recorded, starting from a concentrated solution of **15** in D_2O ($c_1 = 14.25 \cdot 10^{-3}$ M), from which three other solutions were prepared diluting by a factor 6, 9 and 12. The ^1H NMR spectra show that by diluting the solution of complex **15**, the intensity of the signals of the methyl group and of the aromatic protons increases, thus the relative amount of the **11** starting species increases. Thus, based on these

two experiments, it can be assumed that the starting species **11** is formed in a dissociative process. On the other hand, addition of **13** to a solution of **15** (1:1) at weakly acidic pD (5.2) produces more of complex **15**. Furthermore, pD dependent ^1H NMR spectra were recorded, and the conclusions are as follows: At pD = 2 (D_2O , DNO_3) **15** is largely dissociated, and $[\text{Pt}(\text{NH}_3)_3(9\text{-MeA-}N7)]^{2+}$ is already partially protonated at *N1*. If the pD of the aqueous solution of **15** is raised above 8, the concentration of **15** likewise decreases, at the expense of **11** and a new species **15a** (Figure 10).

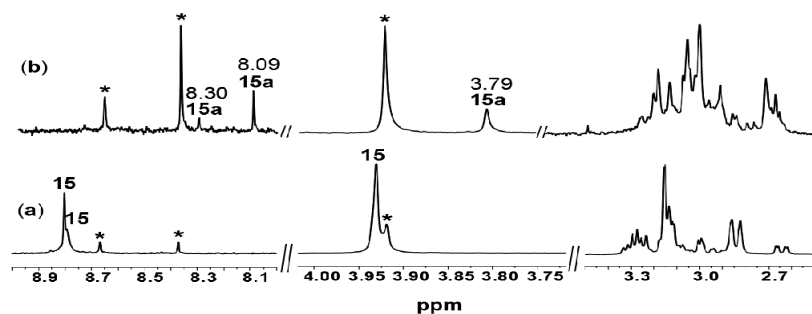
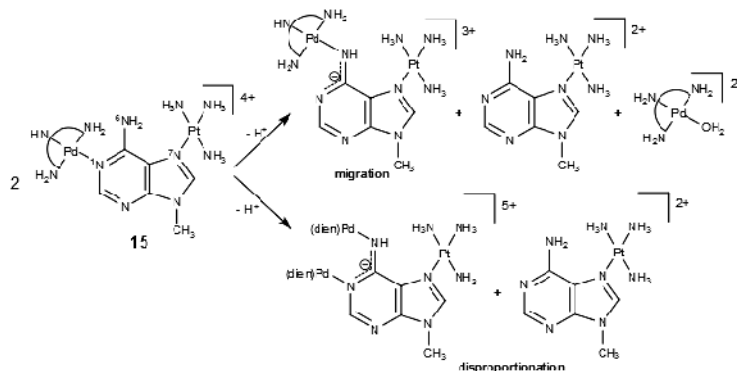


Figure 10. ^1H NMR spectra of **15** in D_2O at pD = 6 (a) and pD = 9.5 (b).

In the ^1H NMR spectrum of complex **15** at pD = 9.5 the presence of the new species **15a** is evident. The chemical shifts of the aromatic protons at 8.30 ppm (s, *H8*) and at 8.30 ppm (s, *H2*), while the signal of the methyl protons at 3.79 ppm can be observed. Using an excess of $\text{Pd}^{\text{II}}(\text{dien})$ (**11**:**13** = 1:2, 1:3, 1:4) in very basic media (pD = 12), the new species **15a** with its CH_3 resonance at 3.79 ppm dominates [18]. The chemical shifts of aromatic proton (*H2*) resonance of **11** precursor complex and of **15a** species can be observed at 8.37 ppm and 8.09 ppm, respectively. Increasing the excess of **13**, the intensity of methyl proton resonance of **15a** (3.79 ppm) against of **11** (3.92 ppm) increases. Concerning the nature of the species **15a** formed from **15** at high pH, two scenarios were considered: Pd migration process from *N1* to *N6*, as previously observed for Pt complexes [19, 25, 26] combined with the dissociation process described above; disproportionation process, which in essence is the product of a reaction between **15** or the migration product with the available $\text{Pd}^{\text{II}}(\text{dien})$ (Scheme 11).



Scheme 11.

The first option is favorable [18], hence **15a** being a migration product, namely $[(\text{dien})\text{Pd}(\text{N}6\text{-}9\text{-MeA}^-\text{-N}7)\text{Pt}(\text{NH}_3)_3]^{3+}$, for the following reasons:

- spectra of **15** recorded at alkaline pD display signals due to free $[\text{Pd}(\text{dien})(\text{OH})]^+$;
- the chemical shifts of the adenine resonances (*H2*, *CH*₃) are closely similar to those of the Pt analogue **16a** (see below), for which Pt migration from *N1* to *N6* is verified.

Solution behavior of **16**

In the ¹H NMR spectrum of **16** in D₂O (*pD* = 6.5), the methyl resonance appears at 3.95 ppm as a sharp singlet, while the two aromatic protons are superimposed at 8.83 ppm. Moreover, the *H8* proton is very much broadened and eventually disappears due to isotopic exchange [18]. In contrast to **15**, complex **16** is not dissociated immediately in D₂O in the *pD* range 4 – 9, at room temperature. However, keeping the solution for six months at room temperature, daylight, *pD* = 6, in the ¹H NMR spectrum of the aged sample, a new CH₃ resonance appears at 3.92 ppm with very low intensity (13% relative to 3.95 ppm resonance), which is assigned to the precursor Pt complex **11**.

In the aged samples kept above *pD* = 9 for days at room temperature the formation of more starting compound is accompanied by the formation of a new species. The ¹H NMR spectra of the aged sample of complex **16** at different *pD* values are presented in **Figure 11**.

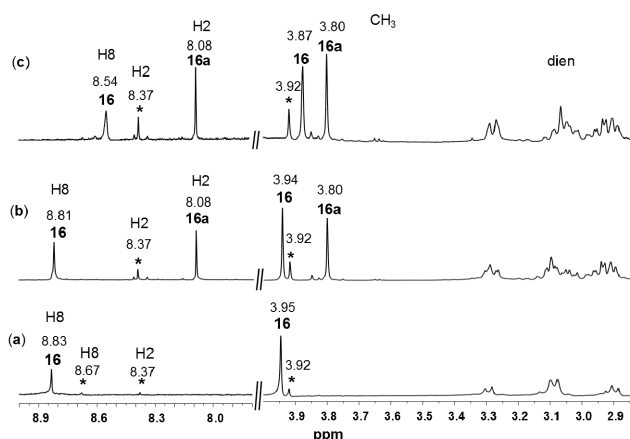


Figure 11. ¹H NMR spectra of complex **16**:
 Aged sample kept for 6 months in D₂O at 22 °C, in daylight, *pD* 6 (a);
 Aged sample brought to *pD* 9 with *pD* dropped to 8.1 within 5 d at 22 °C (b);
 Aged sample brought to *pD* 11 with *pD* dropped to 10.2 within 18 d at 22 °C (c).

Complex **16a** has its aromatic proton resonance at 8.08 ppm (*H2*) and methyl signal at 3.80 ppm, which are upfield shifted relative to those of **16**, as a consequence of

deprotonation of the 9-MeA ligand at *N6* [**19b**, **27**]. The second aromatic adenine proton *H8* is not visible, due to the fast exchange by deuterium. The methylene resonances of the dien ligands are more complicated due to the presence of differently bonded Pt^{II}(dien) entities in **16** and **16a**, respectively. In order to establish the mechanism of formation of a *N1,N6,N7*-trimetalated 9-MeA⁻ species, complex **16** was mixed with [Pd(dien)(D₂O)](ClO₄)₂ in 1:1 ratio on NMR scale. After mixing the reactants, the resulting solution was divided in three parts and the *pH* value of the solutions was adjusted. However, in the ¹H NMR spectra of freshly prepared samples no indication of rapid formation of any additional species is seen. In contrast to the freshly prepared samples, in the case of aged solutions (kept the solutions for weeks to months at room temperature), spectroscopic changes were observed, being accompanied by a drop in *pD*. Thus, in the case of a sample initially adjusted to *pD* = 9 shows a *pD* of 7.5 after five months, while a sample brought initially to *pD* = 12 lowers its *pD* to 9.0 over the same time period.

Solution behavior of 17

Similar to the situation with complex **15**, complex **17** undergoes a dissociation process when dissolved in D₂O (*pD* = 7.4) (Figure 12).

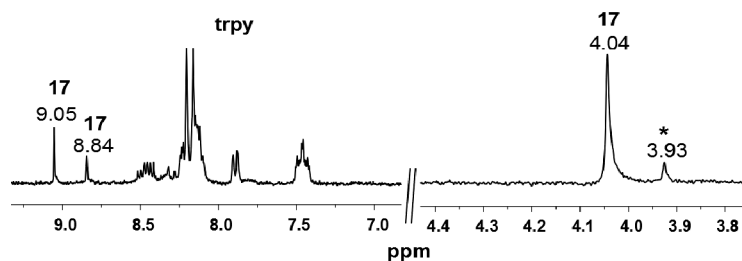
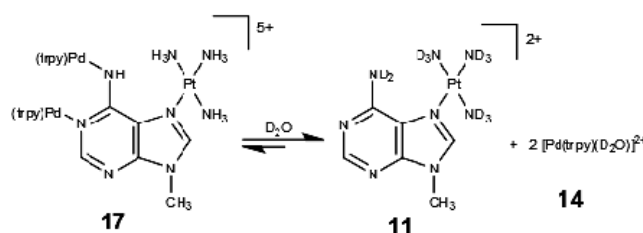


Figure 12. The ¹H NMR spectrum of **17** (freshly prepared sample *pD* = 7.4). Signals due to [Pt(NH₃)₃(9-MeA-N7)]²⁺ (**11**) are indicated by asterisks (*).

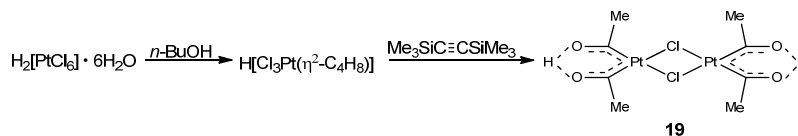
Formation of this compound implies that there is partial loss of both (trpy)Pd^{II} entities from **17**. The dissociation process is presented in the Scheme 12.



Scheme 12.

Going to the alkaline media (*pD* = 9) the dissociation process is more pronounced, thus at *pD* = 12 the dissociation of **17** is practically complete. In the ¹H NMR spectrum of **17**

characterized by Steinborn and collaborators [30] in 1996. The synthesis of the platina- β -diketone (19) is presented in the Scheme 14.



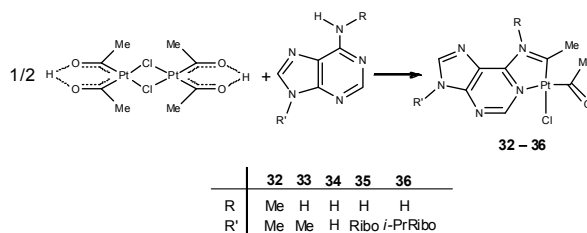
Scheme 14.

Dinuclear platina- β -diketone (19) exhibits an unique reactivity, due to the electronic unsaturation [32]. Therefore, $\text{Pt}_2\{(\text{COMe})_2\text{H}\}_2(\mu\text{-Cl})_2$ was found to react with bidentate nitrogen-donor ligands, like 2,2-bipyridine, 4,4-dimethyl-2,2-bipyridine, 4,4-di(*tert*-butyl)-2,2-bipyridine [33]. Platina- β -diketone (19) can react also with amines: on the one side with amine yielding type complexes which can be considered to be organometallic analogues of platinum blue complexes [34]; on the other side 19 can react with 2-aminopyridines resulting the formation of aminocarbene complexes [35].

Chapter 4.

Synthesis, characterization and reactivity of new adenine based aminocarbene Pt^{II} complexes. Synthesis and characterization of adenine based aminocarbene $\text{Pt}(\text{II})$ complexes 32–36

Based on the literature [35] platina- β -diketone (19) was found to react with two equivalents of adenine derivatives yielding new aminocarbene platinum(II) complexes (Scheme 15).



Scheme 15.

To the yellow suspension of platina- β -diketone (19) in THF at $-78\text{ }^\circ\text{C}$, two equivalents of the corresponding adenine derivative was added and warmed up at room temperature. Reacting overnight, the orange-red complexes 32–36 were obtained in good yields (70 – 80%). They are stable on air both in the solid state and in solution. All complexes are only moderately soluble in the common organic solvents, and insoluble in diethyl ether and pentane. They were characterized by IR and NMR spectroscopy methods. Furthermore, the identities of all complexes were proved by electron spray ionization

Fourier transform ion cyclotron resonance mass spectrometry (ESI-FTICR-MS) and for complex **32**, additionally, by single-crystal X-ray diffraction measurement.

Molecular structure of complexes **32** and **34**

Single crystals of complex **32** suitable for X-ray structure analysis were obtained from CH₂Cl₂ solutions. The molecular structure of complex **32** is shown in **Figure 13**.

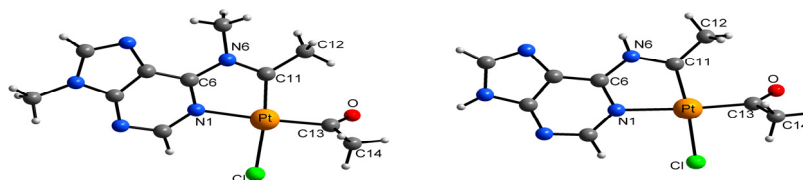


Figure 13. Molecular structure of **32**.

In the molecular structure of complex **32**, the platinum atom is square-planar coordinated by the chelating $\kappa\text{C},\kappa\text{N}$ bound aminocarbene ligand, as well as by an acetyl and a chlorido ligand, thus adopting a primary PtC₂NCl donor set. The five-membered PtC₂N₂ ring is nearly planar and nearly coplanar to the C₅N₄ adenine plane.

¹H NMR spectroscopy of **32–36**

In the ¹H NMR spectrum of complex **32** two signals in the aromatic region and four in the aliphatic region are observed. The coordination of the adenine type ligands gives rise to a downfield shift of resonances of *H2* and *H8* which appear at 8.23 ppm and 9.27 ppm, respectively. Therefore, the two methyl resonances appeared at 4.01 ppm and 4.13 ppm could not be identified. However, the proton resonances of both methyl groups of the adenine ligand are downfield shifted against the free ligand. In the ¹H NMR spectrum (CDCl₃) of the free *N6,N9*-diMeA ligand, resonances of the methyl protons appears at 3.19 ppm (*N6*-CH₃) and 3.79 ppm (*N9*-CH₃). The protons of the methyl group bonded to the carbene C atom and of the carbonyl methyl group were found at 2.18 ppm and 2.46 ppm, respectively (**Figure 14**).

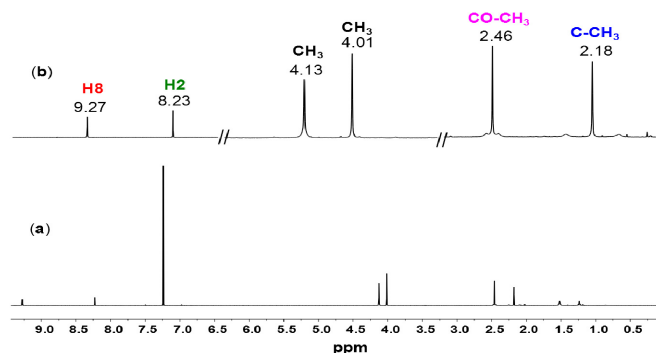


Figure 14. ^1H NMR spectrum of complex **32** (CDCl_3): full spectrum (a); detailed spectrum (b).

In the ^1H NMR spectra of complexes **33–35** the characteristic acetyl protons and the methyl protons bonded to the carbene C atom were found in the expected range. The most characteristic ^1H NMR parameters (δ ppm, J in Hz) for complexes **33–35** are summarized in **Table 1**.

Table 1. δ_{H} (ppm) and $^3J_{\text{Pt,H}}$ (in Hz; given in parentheses) for complexes **33–35**.

	33 ^a	34 ^b	35 ^c
H^2	8.43	8.54	8.93
H^8	9.01	9.18	9.22
COCH_3	2.50 (14.2)	2.42 (14.2)	2.49 (20)
CCH_3	1.23 ^d	2.24 (58)	1.98 (35)

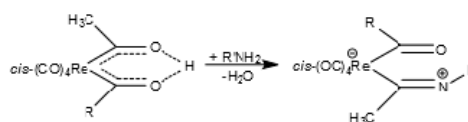
a) In CDCl_3 . b) In CD_3NO_2 . c) CD_3OD d) Coupling not observed.

^{13}C NMR spectrum of complex **36**

In fully agreement with the ^1H NMR of complex **36**, in the ^{13}C NMR spectrum two highly downfield shifted ^{13}C resonances were found, one of them for the carbene C atom at 227.5 ppm and one for the acetyl C atom at 220.0 ppm. Furthermore, the ^{13}C resonance of the methyl C atom bound to the carbene C atom was found nearby the corresponding resonances of aminocarbene type complexes (33.4 versus 32.5/31.9 ppm) [35]. In order to identify each carbon atoms of the sugar part of the complex, ^{13}C NMR spectrum in APT mode was recorded.

Synthesis and characterization of Pt^{II} containing ketoimine complexes

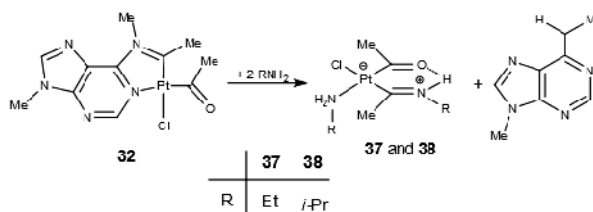
In 1978 Lukehart and Zeile found that reacting metalla-β-diketone molecules, like *cis*-(OC)₄Re[C(CH₃)O⋯H⋯OC(R)] (R = Me, *i*-Pr) with anhydrous ammonia or primary aliphatic or aromatic amines leads to the formation of metalla-β-ketoimine molecules (**Scheme 16**) [36].



Scheme 16.

Concerning the reactivity of the adenine based aminocarbene complexes it was found that reacting with primary alkyl amines, the first platinum-β-ketoimines were obtained.

Therefore, reacting complex **32** with two equivalents of ethyl- and *i*-Pr-amine the platinum-β-ketoimines, namely [Pt(RNH₂)Cl]{(COMe){C(NR)Me}H} (R = Et/*i*-Pr; **37/38**) were obtained (**Scheme 17**).



Scheme 17.

The white compounds were obtained in good yields (ca. 75%). They are stable on air both in the solid state and in solution. These ketoimine complexes are soluble in CHCl₃ and CH₂Cl₂, and they are insoluble in diethyl ether and pentane. They were characterized by NMR spectroscopy (¹H, ¹³C and ¹⁹⁵Pt), IR, and by ESI-FTICR-MS. Furthermore, DFT calculations were performed.

Structural investigation of complexes **37** and **38** by NMR spectroscopy

In the ¹H NMR spectra the signals of all protons were found in the expected range with correct intensities. The ¹H NMR spectrum of complex **37** is presented in **Figure 15**. In the ¹H NMR spectrum of complex the most relevant proton resonances of the C(O)CH₃ and C(NHEt)CH₃ groups appear at 2.74 and 1.95 ppm, respectively. The resonances of the acetyl protons are superimposed with that of the methylene protons of the unreacted (excess) of ethylamine.

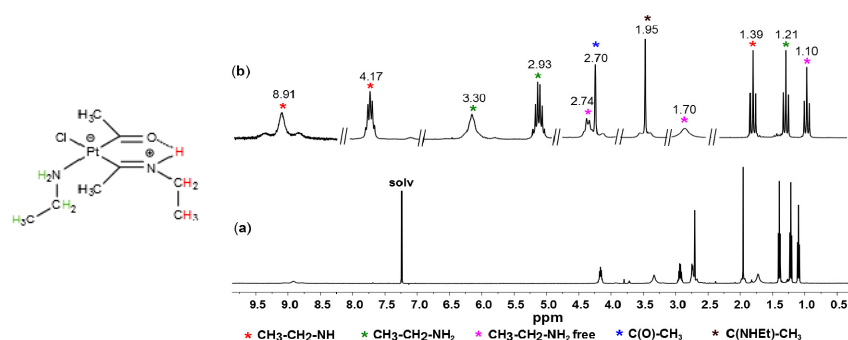


Figure 15. ^1H NMR spectra of complex **37** (CDCl_3): full spectrum (a); detailed spectrum (b).

In both cases the most downfield shifted resonances are observed for the $\text{CH}_3\text{CH}_2\text{NH}$ group ($-\text{CH}_2/-\text{CH}_3$; 4.17/1.39 ppm). However, the correlation between the different kind of protons of the same group was proved by $^1\text{H}-^1\text{H}$ COSY measurement. The $^1\text{H}-^1\text{H}$ COSY spectrum of complex **37** shows the correlation between the resonances at 4.17/1.39 ppm and 2.93/1.21 ppm, which most probably corresponds to the methylene and methyl protons of $\text{CH}_3\text{CH}_2\text{NH}$ and coordinated $\text{CH}_3\text{CH}_2\text{NH}_2$ groups, respectively.

In the ^1H NMR spectrum of complex **38** the most relevant proton resonances of $\text{C}(\text{O})\text{CH}_3$ and $\text{C}(\text{NiPrH})\text{CH}_3$ groups appear at 2.69 and 1.97 ppm, with coupling constants $^3J_{\text{Pt,H}} = 36.4$ and 21.9 Hz, respectively. The broad signals of the different type of amino groups: $-\text{NH}/-\text{NH}_2$ at 8.39/2.87 ppm with correct intensities can be assigned. Furthermore, the resonances of the methylenic protons of the tree type of amines are identified at 5.16, 3.33 and 3.17 ppm, while the resonances of the methyl protons has their chemical shifts in the range of 1.40 – 1.12 ppm.

In the ^{13}C NMR spectrum of complex **37** the corresponding C signals are observed in the expected range (Figure 16).

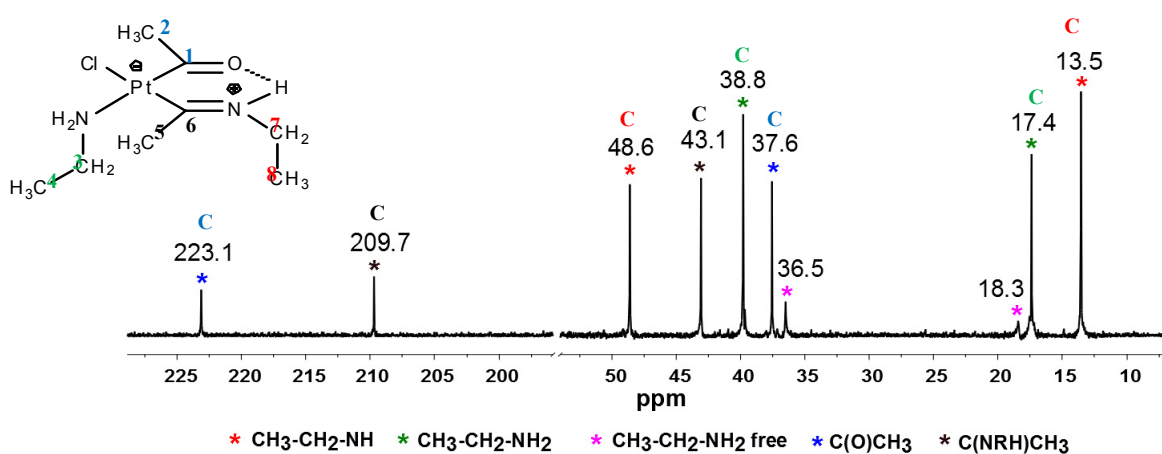


Figure 16. ^{13}C NMR spectrum of complex **37**.

In the ^{13}C NMR spectrum of complex **37** the corresponding C signals are observed in the expected range. The two most downfield shifted resonances correspond to the carbonyl group of the acetyl and to the $\text{C}(\text{NEtH})\text{-CH}_3$ ligands. From the gHMBC spectrum of complex **37** the correlation between the C resonance/proton resonance at 223.1/2.70 ppm and 209.7/1.95 ppm are evident, which corresponds to the $\text{C}(\text{O})\text{CH}_3$ and $\text{C}(\text{NEtH})\text{CH}_3$ groups, respectively. Furthermore, the correlation between of the methyl and methylene groups of the alkyl group were identified as follows: 1.21/38.8 ppm and 1.39/48.6 ppm, which correspond to the coordinated ethyl amine group and to the noncoordinated $\text{CH}_3\text{CH}_2\text{NH-}$ group, respectively. According to the $^{13}\text{C}\text{-}^1\text{H}$ COSY and gHMBC measurements, it can be assumed that the resonances of the methyl and methylene C atoms of the coordinated ethylamine group appeared at 17.4 and 38.8 ppm, while for the noncoordinated $\text{CH}_3\text{CH}_2\text{NH-}$ group at 13.5 and 48.6 ppm.

Similar to the complex **37**, in the ^{13}C NMR spectrum of complex **38** the most downfield shifted resonance corresponds to the carbonyl group of the acetyl ligand (220.4 ppm; while for the $\text{C}(\text{NiPrH})\text{-CH}_3$ group the C resonance appears at 209.8 ppm. Furthermore, the resonances of the methyl C atom at 43.0 ppm were assigned to the $\text{C}(\text{NiPrH})\text{CH}_3$, while the resonance appeared at 37.0 ppm to the $\text{C}(\text{O})\text{CH}_3$ ligand, confirmed by $^{13}\text{C}\text{-}^1\text{H}$ COSY and gHMBC measurements.

General conclusions

The first part of the original contributions (Chapter 2) is concerned with the synthesis and characterization of new di- and trimetalated species of 9-MeA. Therefore, the synthesized complexes **15-17** were characterized both in the solid state, by X-ray diffraction, and in the D₂O solution by ¹H NMR and ¹⁹⁵Pt NMR spectroscopy. The solution behaviour of complexes **15-17** shows different processes, like metal migration from *N1* to *N6* atom of 9-MeA (**15** and **16**), and decomposition (**17**). Furthermore, DFT calculations on **15** and **17** were carried out. The original contributions presented in the second part of this thesis (Chapter 4) describes the synthesis and characterization of some new adenine based aminocarbene complexes. The aminocarbene complexes **32-36** were obtained from the reaction of platina-β-diketone and adenine or its derivatives, such as 9-MeA, adenosine, 2'3'-isopropylidene adenosine, *N6*-Me,9-MeA.

The reactivity of these aminocarbene complexes were tested, thus found that they can react with different primer amines, like ethyl amine and isopropyl amine. Therefore, the first Pt contained ketoimine complexes were obtained. The ketoimine complexes **37** and **38** were obtained in pure state and characterized by ¹H NMR, ¹³C NMR, ¹⁹⁵Pt NMR spectroscopy, and by ESI-HRMS. Furthermore, DFT calculations were performed.

List of synthesized compounds

1. [(dien)Pd(*NI-9-MeA-N7*)Pt(NH₃)₃](ClO₄)₄·9.33H₂O (15)
2. [(dien)Pt(*NI-9-MeA-N7*)Pt(NH₃)₃](ClO₄)₄·H₂O (16)
3. [{(trpy)Pd}₂(*NI,N6-9-MeA-N7*)Pt(NH₃)₃](ClO₄)₅·3H₂O (17)
4. [Pt(COMe)Cl{CMe(*N6-Me,9-MeA*⁻)-κC,κN}] (32)
5. [Pt(COMe)Cl{CMe(*N6-H,9-MeA*⁻)-κC,κN}] (33)
6. [Pt(COMe)Cl{CMe(*N6-H,9-HA*⁻)-κC,κN}] (34)
7. [Pt(COMe)Cl{CMe(*N6-H,9-RiboA*⁻)-κC,κN}] (35)
8. [Pt(COMe)Cl{CMe(*N6-H,9-*i*-PrRiboA*⁻)-κC,κN}] (36)
9. [Pt(EtNH₂)Cl{(COMe){C(N-Et)Me}H}] (37)
10. [Pt(*i*PrNH₂)Cl{(COMe){C(N-*i*Pr)Me}H}] (38)

List of publications

1. Timea Mihály, Marta Garijo Añorbe, Francisca M. Albertí, Pablo J. Sanz Miguel, Bernhard Lippert, Multiple Metal Binding to the 9-Methyladenine Model Nucleobase Involving N1, N6, and N7: Discrete Di- and Trinuclear Species with Different Combinations of Monofunctional Pd^{II} and Pt^{II} Entities *Inorg. Chem.*, **2012**, *51*, 10437–10446.
2. Francisca M. Albertí, Timea Mihály, Bernhard Lippert, Pablo J. Sanz Miguel, Unsupported single-walled water cluster nanotube: A novel hydrogen bonding pattern for water organization, *CrystEngComm*, **2012**, *14*, 6178–6181.
3. Timea Mihály, Martin Bette, Béla Mihály, Jürgen Schmidt, Harry Schmidt, Dirk Steinborn, Synthesis, structure and characterization of adenine-based aminocarbene complexes of platinum(II), *J. Organomet. Chem.*, **2013**, *739*, 57–62.
4. Csaba Fábri, Edit Mátyus, Tibor Furtenbacher, László Nemes, Béla Mihály, Timea Zoltáni, Attila G. Császár, Variational quantum mechanical and active database approaches to the rotational-vibrational spectroscopy of ketene, H₂CCO, *Journal of Chemical Physics* **2011**, *135*, 094307-1 – 094307-19.

Bibliography of the summary

1. R. Dahm, *Developmental Biology*, **2005**, 278, 274.
2. J.D. Watson, F.H.C. Crick, *Nature*, **1953**, 171, 737.
3. B. Lippert, *Cisplatin: chemistry and biochemistry of a leading anticancer drug*, Wiley-VCH Weinheim, **1999**.
4. B. Rosenberg, L. VanCamp, J.E. Trosko, V.H. Mansour, *Nature*, **1969**, 222, 385.
5. H.T. Chifotides, K.R. Dunbar, *Acc. Chem. Res.*, **2005**, 38, 146.
6. B. Lippert, *Coord. Chem. Rev.*, **2000**, 200-202, 487.
7. M.J. McCall, M.R. Taylor, *Biochim. Biophys. Acta.*, **1975**, 390, 137.
8. C. Meiser, B. Song, E. Freisinger, M. Peilert, H. Sigel, B. Lippert, *Chem. Eur. J.*, **1997**, 3, 388.
9. F. Zamora, M. Kunsman, M. Sabat, B. Lippert, *Inorg. Chem.*, **1997**, 36, 1583.
10. J. Arpalahti, K.D. Klika, *Eur. J. Inorg. Chem.*, **1999**, 1199.
11. M.J. McCall, M.R. Taylor, *Biochim. Biophys. Acta.*, **1975**, 390, 137.
12. F. Schwarz, B. Lippert, *Inorg. Chim. Acta.*, **1990**, 176, 113.
13. A. Terzis, *Inorg. Chem.* **1976**, 15, 793.
14. S. Jaworski, S. Menzer, B. Lippert, M. Sabat, *Inorg. Chim. Acta*, **1993**, 205, 31.
15. M.S. Lüth, E. Freisinger, F. Glahé, J. Müller, B. Lippert, *Inorg. Chem.*, **1998**, 37, 3195.
16. A. Schreiber, E.C. Hillgeris, A. Erxleben, B. Lippert, *Z. Naturforsch.*, **1993**, 48b, 1603.
17. X. Zhu, E. Rusanov, R. Kluge, H. Schmidt, D. Steinborn, *Inorg. Chem.*, **2002**, 41, 2667.
18. T. Mihály, M. Garijo Añorbe, F.M. Albertí, P.J. Sanz Miguel, B. Lippert, *Inorg. Chem.*, **2012**, 51, 104.
- 18a. It must to be mentioned, that complex **18** is part of the PhD thesis of M. Garijo Añorbe, but published in Ref. 18. Thus, the structure of **18** was used in this work just for comparison. The DFT calculations on this compound is part of the original contributions of the present thesis.
19. (a) S. Ibañez, F.M. Albertí, P.J. Sanz Miguel, B. Lippert, *Inorg. Chem.*, **2011**, 50, 10439. (b) M. Garijo Anorbe, T. Welzel, B. Lippert, *Inorg. Chem.*, **2007**, 46, 8222.
20. E.G. Talman, W. Brunig, J. Reedijk, A.L. Spek, N. Veldman, *Inorg. Chem.*, **1997**, 36, 854.
21. N. Hadjiliadis, T. Theophanides, *Inorg. Chim. Acta*, **1976**, 16, 67.

22. R. Beyerle-Pfnür, S. Jaworski, B. Lippert, H. Schöllhorn, U. Thewalt, *Inorg. Chim. Acta*, **1985**, *107*, 217.
23. G.W. Watt, W.A. Cude, *Inorg. Chem.*, **1968**, *7*, 335.
24. R. Karkalić, Ž.D. Bugarčić, *Monatshefte für Chemie*, **2000**, *131*, 819.
25. J. Arpalahti, K.D. Klika, S. Molander, *Eur. J. Inorg. Chem.*, **2000**, 1007 and refs. cited.
26. M. Garijo Anorbe, M.S. Lüth, M. Roitzsch, M. Morell Cerdà, P. Lax, G. Kampf, H. Sigel, B. Lippert, *Chem. Eur. J.*, **2004**, *10*, 1046.
27. It is note that there is a typing error in Figure 2 of ref. **19b**: The assignment of the two methyl resonances between 3.5 and 4 ppm needs to be reversed. The assignment of the H2 resonances is correct. See in ref. **18**.
28. (a) C.M. Lukehart, *Acc. Chem. Res.*, **1981**, *14*, 109.
(b) C. M. Lukehart, *Adv. Organomet. Chem.*, **1986**, *25*, 45.
29. C.M. Lukehart, G.P. Torrence, *Inorg. Chem.*, **1979**, *18*, 3150.
30. D. Steinborn, M. Gerisch, K. Merzweiler, K. Schenzel, K. Pelz, H. Bögel, J. Magull, *Organometallics*, **1996**, *15*, 2454.
31. M.A. Garralda, R. Hernández, L. Ibarlucea, E. Pinilla, M. R. Torres, *Organometallics* **2003**, *22*, 3600.
32. D. Steinborn, *Dalton Trans.*, **2005**, 2664.
33. M. Gerisch, C. Bruhn, A. Vyater, J.A. Davies, D. Steinborn, *Organometallics* **1998**, *17*, 3101.
34. D. Steinborn, M. Gerisch, F.W. Heinemann, C. Bruhn, *Chem. Commun.*, **1997**, 843.
35. T. Gosavi, C. Wagner, K. Merzweiler, H. Schmidt, D. Steinborn, *Organometallics*, **2005**, *24*, 533.
36. C.M. Lukehart, J.V. Zeile, *Inorganic Chemistry*, **1978**, *17*, 2369.